



Towards Automatic Visual Sea Grass Detection in Underwater Areas of Ecological Interest

Antoni Burguera, Francisco Bonin-Font, Jose Luis Lisani, Ana Belen Petro and Gabriel Oliver

Dept. Matemàtiques i Informàtica - Universitat de les Illes Balears

Ctra. Valldemossa Km. 7,5 - 07122 Palma de Mallorca (SPAIN)

{antoniburguera, francisco.bonin, josluis.lisani, anabelen.petro, goliver}@uib.es

Abstract—In areas of ecological interest, the detection and control of seaweed such as *Posidonia Oceanica* is usually performed by divers. Due to the limited capacity of the scuba tanks and the human security protocols, this task involves several short immersions leading to poor temporal and spatial data resolution. Thus, it is desirable to automate this task by means of underwater robots. This paper describes a method to autonomously detect *Posidonia Oceanica* in the imagery gathered by an underwater robot. The proposed approach uses a set of Gabor filters to characterize an image. This characterization is used to detect the regions containing seaweed by means of a Support Vector Machine. The experiments, conducted with an Autonomous Underwater Robot in several marine areas of Mallorca, show promising results towards the automated seafloor classification from extended video sequences.

I. INTRODUCTION

The preservation of the marine biodiversity is crucial for many industrial and touristic activities as well as an important goal of the Horizon 2020. Such preservation involves, among many other tasks, seabed monitoring in order to map certain species of seaweed. In the Mediterranean, mapping both the endemic *Posidonia Oceanica* (P.O.) and invasive species such as *Caulerpa Taxifolia* is becoming more and more important. As a matter of fact, invasive species are considered one of the major threats to biodiversity.

The P.O. forms large underwater meadows that protect the shoreline against the erosion by attenuating both marine currents and waves. It is the source of food and shelter for many organisms and, by absorbing large amounts of carbon, it increases the quality and transparency of the water [3]. Besides, the European Commission's directive 92/43/CEE states that P.O. is a priority natural habitat. Consequently, monitoring and mapping P.O. is of crucial importance.

Nowadays, the task of monitoring of P.O. is typically achieved by human divers, similarly to the monitoring and flaw detection in submerged industrial structures [14]. They photograph the meadows and measure their extension by means of markers and gauges installed in the perimeter. Acoustic localization can be used to recover the diver position and, thus, to georeference the gathered data [15]. However, these

This work is partially supported by Ministry of Economy and Competitiveness under contracts TIN2014-58662-R, DPI2014-57746-C3-2-R and FEDER funds.

approaches are not only slow and inaccurate, but also limited in time by the scuba air tanks capacity.

Recent strategies include the use of multi-spectral satellite imagery [10] or acoustic bathymetry [11]. However, these approaches have important flaws when trying to discriminate P.O. from other algae types. Lately, some researchers [16] have explored the use of *Autonomous Underwater Vehicles* (AUV) endowed with cameras. However, at the extent of the authors knowledge, the automatic detection and mapping of P.O. has not been achieved.

The *Augmented Reality Sub-sea Exploration Assistant* (AR-SEA) is a funded Spanish project aimed at facilitating underwater monitoring using AUVs and *Remotely Operated Vehicles* (ROV). One of the project goals is to autonomously or semi-autonomously map P.O. meadows and build photo-realistic 3D mosaics of the mapped environment to control their state and evolution. Other goals include monitoring and mapping underwater sewage pipes and submerged industrial structures. This paper focuses on the process of image characterization, training and classification being developed in the aforementioned project to detect P.O. from underwater imagery, although the presented approach is of direct application in the mentioned industrial context.

This process involves three tasks. First, the underwater imagery is improved using color correction and image enhancement algorithms, as described in Section II. Second, a set of Gabor filters is used to describe the enhanced images as presented in Section III. Finally, a supervised learning schema, explained in Section IV, is used to detect the P.O.

Section V shows the preliminary results obtained from several video sequences recorded by an AUV in several coastal areas of Mallorca.

II. COLOR CORRECTION AND IMAGE ENHANCEMENT

The water column between the camera and the sea-floor induces several effects on the obtained images such as attenuation and scattering. Light attenuation depends on the light frequency, typically producing a loss of red tonalities. Scattering usually reduces the contrast and may be responsible for blur in the image. Additionally, these effects are conditioned by the water salinity and the existence of suspended particles. In order to recover the actual color of underwater imagery it is crucial to take into account the aforementioned effects as well as the 3D geometry of the scene [1]. However, the aim

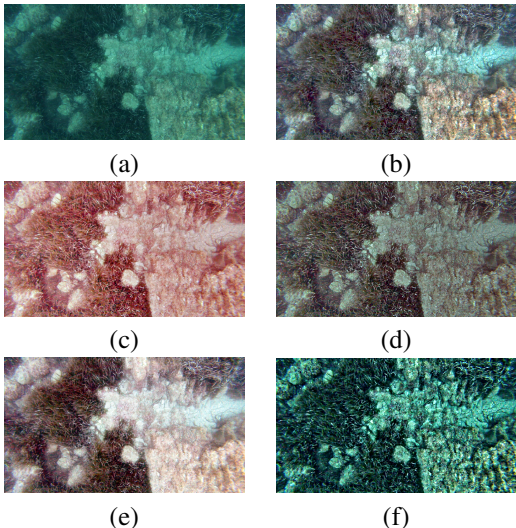


Fig. 1. Examples of image enhancement. (a) Original image. (b) LCC. (c) MSR. (d) MSR-NK. (e) Mai (f) Guided filter.

of this paper is not to recover the actual scene colors but to enhance color, contrast and texture in order to facilitate further P.O. detection.

In this study, we apply several outstanding color and contrast enhancement algorithms to the images gathered by our AUV. Our goal is to analyze their suitability to improve the image classification process.

The first of the tested approaches is a local gamma correction method: the *Local Color Correction* (LCC) [12]. The second one is the *Multi Scale Retinex* (MSR) [6], which is a center/surround method with a Gaussian kernel. The third one, the *Multi Scale Retinex - New Kernel* (MSR-NK) [13], improves the MSR with a new kernel responsible for a good trade-off between scale invariance and integrability. The fourth method [9] is a tone mapping algorithm based on [7]. In the context of this paper, this method will be referred to as the *Mai* method. Finally, the fifth method is a pure guided filter [4]. All these methods are applied separately to each color channel followed by a contrast-limited adaptive histogram equalization.

These algorithms have been successfully tested on air. In particular, the first four methods have been selected because they obtained the best scores in a benchmark for contrast enhancement in satellite imagery [8]. However, at the extent of the authors knowledge, their effects on underwater images has not been quantified before. Moreover, this is the first study involving these image enhancement techniques to detect P.O.

Figure 1 shows the effects of the aforementioned methods when applied to an image of the sea-floor. As stated before, these enhancement methods are not aimed at recovering the actual sea-floor colors. Their goal is to improve the P.O. detection ratio when using the description and classification approaches presented in the next sections.

III. IMAGE DESCRIPTORS

This Section presents our approach to compute the image descriptors that will be subsequently used to perform the

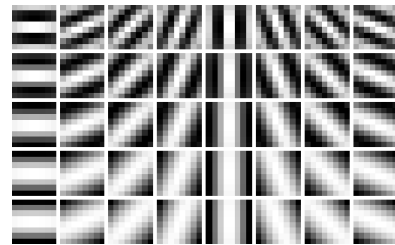


Fig. 2. The real part of the 40 Gabor filters used. Each row corresponds to a different scale and each column to a different orientation.

image classification. Our proposal begins by down-sampling the enhanced color images to a resolution of 640×480 pixels. Afterwards, the image is divided into a set of 400 sub-images or patches of 32×24 pixels. A descriptor is computed for each of these patches by means of 2D Gabor filters. Gabor filters were chosen because they have predominant orientations, similarly to the P.O. leaves and, thus, they are likely to provide a strong response in front of P.O.

Gabor filters approximate some characteristics of the primary visual cortex of mammals. Also, they have been successfully used to perform image segmentation and object classification [5]. A Gabor filter is a sinusoidal plane wave modulating a Gaussian kernel function and can be formulated as follows:

$$h(x, y) = e^{-\frac{1}{2}(\frac{x^2}{\sigma_x^2} + \frac{y^2}{\sigma_y^2})} e^{-j2\pi(u_0x+v_0y)} \quad (1)$$

where (u_0, v_0) defines the central frequency and (σ_x, σ_y) denotes the standard deviation of the Gaussian kernel.

Our proposal is to generate a bank of 40 Gabor filters, involving 8 different orientations and 5 different scales and discretizing each filter to an 8×8 matrix. Figure 2 depicts the real part of the filter bank used in this paper.

The red, green and blue channels of each patch are convolved with all the filters in the filter bank. From each convolution, two significant values are extracted. On the one hand, the local energy, defined as follows:

$$E = \sum_{i=0}^{m-1} \sum_{j=0}^{n-1} c(i, j)^2 \quad (2)$$

where m and n are the number of rows and columns, respectively, of c , which is the result of the convolution.

On the other hand, the amplitude is also computed for each color channel of each patch as follows:

$$A = \sum_{i=0}^{m-1} \sum_{j=0}^{n-1} |c(i, j)| \quad (3)$$

Being each color channel convolved with 40 Gabor filters, a patch descriptor is composed of 240 values.

IV. PATCH CLASSIFICATION

Our proposal is to use a *Support Vector Machine* (SVM) [2] to perform the patch classification. Two classes are defined to

| | Raw | LCC | MSR | MSR-NK | Mai | Guided |
|----------|-----|-------|-------|--------|-------|--------|
| μ | 91% | 91.1% | 91.7% | 92.6% | 92.9% | 91.8% |
| σ | 2.3 | 1.8 | 1.7 | 1.3 | 1.1 | 1.7 |

TABLE I

MEAN (μ) AND STANDARD DEVIATION (σ) OF THE P.O. DETECTION HIT RATIO.

train the SVM. These classes, named 0 and 1, denote patches not containing P.O. and patches containing P.O. respectively. Accordingly, the P.O. detection is binary at the patch level.

The SVM is trained using binary hand-labeled images as ground truth. However, taking into account that in some images it was difficult to clearly state the P.O. perimeter, the SVM is trained under the assumption that a 5% of the training samples are outliers.

V. EXPERIMENTAL RESULTS

In order to perform the experiments, a dataset of 69 color images, together with their corresponding ground truth, was used. These images belong to six video sequences gathered by the bottom-looking camera of our AUV during different missions in several coastal areas of Mallorca. These images involve different illumination conditions and different types of P.O. textures. One third of the images in the dataset has only P.O. Another third has no P.O. at all, and the last third contains patches with P.O. and patches without it.

A. Quantitative results

The following experimental setup has been used to quantify the quality of the proposed image classification schema and to evaluate the influence of the image enhancement methods.

First, all the images in the dataset have been processed using each of the methods described in Section II. Then, a 20% of each group of enhanced images has been randomly selected as the training set, and the remaining 80% as the test set.

Second, the descriptors presented in Section III have been computed for each training set. These descriptors, together with the ground truth information, have been used to train the SVM described in Section IV.

Third, the descriptors have also been computed for the test sets and classified using the trained SVM. The quality of the classification has been assessed thanks to the ground truth.

These steps have been repeated 500 times for each image enhancement technique and also using the non enhanced images. Due to the random nature of the training and test sets selection, these sets change at each trial. Thus, we have performed a Monte Carlo cross-validation. Thanks to this, we have information about the hit ratio of the P.O. detection for each image enhancement technique.

Figure 3 and Table I show the obtained results. As it can be observed, the best results are achieved when enhancing the images using the Mai method. In this case, a 92.9% of the patches were correctly classified. It can also be observed that all the methods improve the mean hit ratio with respect to the use of unprocessed imagery, although the LCC improvement is small.

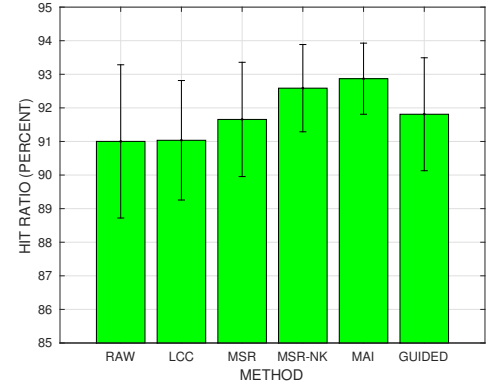


Fig. 3. Mean and standard deviation of the P.O. detection hit ratio for each of the image enhancement methods.

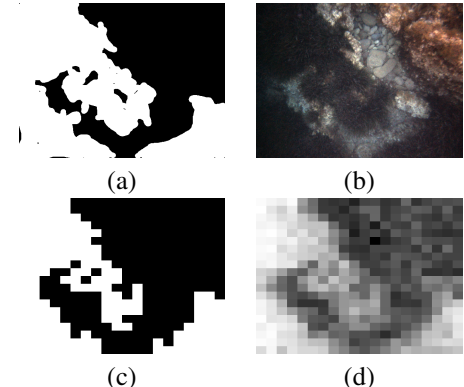


Fig. 4. Example of the obtained results. (a) Ground truth. White areas denote P.O. (b) Image under analysis. (c) Classification result. White areas denote P.O. (d) SVM scores.

As for the hit ratio standard deviation, it provides information about the training robustness in front of different training sets. A large standard deviation is the result of significant differences during the classification process depending on the specific training set. To the contrary, a small standard deviation suggests that different training sets barely influence the resulting hit ratio.

From this point of view, Mai method is also the most robust, being $\sigma_{Mai} = 1.1$. Also, all the methods improve the robustness with respect to the use of raw imagery. Moreover, LCC, which is similar to the use of unprocessed images when observing the mean hit ratio, leads to an important improvement when the standard deviation is taken into account, as shown in Table I.

B. Qualitative results

Next, some examples of the classification results are shown. As the quantitative data suggests that Mai method is the one that provides a better hit ratio, the examples are based on this method.

Figure 4-b shows an image with P.O. and two different types of background (gray and brown). Due to the bad illumination conditions, the P.O. appears with a very dark tonality.

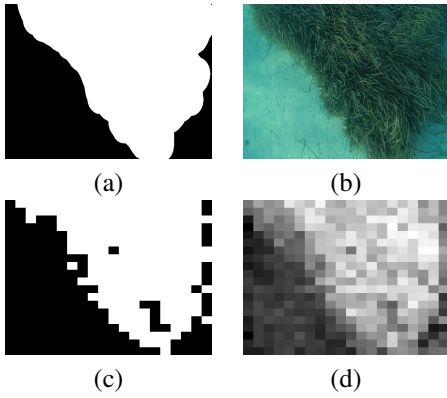


Fig. 5. Example of the obtained results. (a) Ground truth. White areas denote P.O. (b) Image under analysis. (c) Classification result. White areas denote P.O. (d) SVM scores.

The manually labeled ground truth is shown in Figure 4-a. The classification results, depicted in Figure 4-c are almost coincident with the ground truth, except for the resolution, as classification is binary at the patch level. For the sake of completeness, Figure 4-d shows the resulting SVM scores. These scores are related to the distance from each patch feature vector to the hyperplane constructed during the SVM training to separate the classes.

Figure 5 shows the same data for a different image. It can be observed that P.O. color may change significantly from one image to another, having a much clear green tonality in this case. Even in these cases, the presented approach is able to successfully detect P.O. independently of the differences between the images.

VI. CONCLUSION

In this paper, a method to autonomously detect P.O. in underwater imagery has been presented and experimentally validated. The method consists of three steps. First, each image is enhanced and divided in 400 patches. Second, a descriptor based on Gabor filters is computed for each patch. Finally, a previously trained SVM classifies the patch using the descriptor.

A Monte Carlo cross-validation schema has been used to determine which of the five proposed image enhancement methods leads to better results. The results suggest that the Mai method is the best both in terms of mean hit ratio and robustness. Additionally, two examples of the classification results have been shown.

The significant progress reached in the development of the technique and the success rate obtained with video sequences grabbed in real marine scenarios, let us determine that the technology reaches a TRL of 6 according to the H2020 work program.

VII. FUTURE WORK

Even though the results show a very high hit ratio, as almost the 93% of the patches have been correctly classified, there are some points that deserve further research.

On the one hand, the image enhancement methods should be adapted to take into account the particularities of underwater imaging. On the other hand, values other than local energy and amplitude should be tested when building the descriptors. Also, other machine learning techniques, such as neural networks, should be tested and compared to the SVM. Finally, using overlapping patches and considering detection neighborhood could improve the classification results.

Additionally, our forthcoming objective is to classify P.O. in more extended areas, covering complete meadows of several squared kilometers, in order to obtain 2D mosaics of classified frames, and to calculate automatically all biological parameters needed to evaluated their extension and conservation state, reaching a TRL of 7.

REFERENCES

- [1] M. Bryson, M. Johnson-Robertson, O. Pizarro, and S. Williams, "True Color Correction of Autonomous Underwater Vehicle Imagery," *Journal of Field Robotics*, pp. 1–22, 2015.
- [2] N. Cristianini and J. Shawe-Taylor, *An Introduction to Support Vector Machines*. Cambridge University Press, 2000.
- [3] E. Diaz-Almela and C. Duarte, "Management of Natura 2000 Habitats 1120, (Posidonia Oceanicae)," European Commission, Tech. Rep., 2008.
- [4] K. He, J. Sun, and X. Tang, "Guided Image Filtering," *IEEE Transactions on Pattern Analysis and Machine Intelligence*, vol. 35, no. 6, pp. 1397–1409, 2013.
- [5] A. Jain, N. Ratha, and S. Lakshmanan, "Object Detection Using Gabor Filters," *Pattern Recognition*, vol. 30, no. 2, pp. 295–309, 1997.
- [6] D. Jobson, Z. Rahman, and G. Woodell, "A Multiscale Retinex for Bridging the Gap Between Color Images and the Human Observation of Scenes," *IEEE Transactions on Image Processing*, vol. 6, no. 7, pp. 965–976, 1997.
- [7] P. Lauga, G. Valenzise, G. Chierchia, and F. Dufaux, "Improved Tone Mapping Operator for HDR Coding Optimizing the Distortion/Spatial Complexity Trade-off," in *Proceedings of IEEE, European Signal Processing Conference*, September 2014, pp. 1607–1611.
- [8] J. Lisani, J. Michel, J.-M. Morel, A. Petro, and C. Sbert, "An inquiry of contrast enhancement methods for satellite image," *Submitted to IEEE Transactions on Geoscience and Remote Sensing*, 2016.
- [9] Z. Mai, H. Mansour, R. Mantiuk, P. Nasipoulous, R. Ward, and W. Heidrich, "Optimizing a tone curve for backward-compatible high dynamic range image and video compression," *IEEE Transactions on Image Processing*, vol. 20, no. 6, pp. 1558–1571, 2011.
- [10] R. Matarrese, M. Acquaro, A. Morea, K. Tijani, and M. Chiaradia, "Applications of Remote Sensing Techniques for Mapping Posidonia Oceanica Meadows," in *Proceedings of IEEE International Geoscience and Remote Sensing Symposium*, 2008, pp. 906–909.
- [11] M. Montefalcone, A. Rovere, V. Parravicini, G. Albertelli, C. Morri, and C. N. Bianchi, "Evaluating Change in Seagrass Meadows: A time-framed Comparison of Side Scan Sonar Maps," *Aquatic Botany*, vol. 104, pp. 204–212, 2013.
- [12] A. Moore, J. Allman, and R. M. Goodman, "A Real-time Neural System for Color Constancy," *IEEE Transactions on Neural Networks*, vol. 2, no. 2, pp. 237–246, 1991.
- [13] J. Morel, A. B. Petro, and C. Sbert, "What is the Right Center/Surround for Retinex?" in *Proceedings of the International Conference on Image Processing (ICIP)*, 2014.
- [14] A. Ortiz, J. Antich, and G. Oliver, "A particle filter based approach for tracking undersea narrow telecommunication cables," *Machine Vision and Applications*, vol. 22, no. 2, pp. 283–302, 2011.
- [15] D. Scaradozzi, G. Conte, G. de Capua, L. Sorbi, C. Luciani, P. de Cecco, and A. Sorci, "Innovative Technology for Studying Growth Areas of Posidonia Oceanica," in *Proceedings of the IEEE WorkShop on Environmental, Energy and Structural Monitoring Systems.*, 2009, pp. 71–75.
- [16] A. Vasiljevic, N. Miskovic, Z. Vukic, and F. Mandic, "Monitoring of Seagrass by Lightweight AUV: A Posidonia Oceanica Case Study Surrounding Murter Island of Croatia," in *Mediterranean Conference on Control and Automation (MED)*, June 2014, pp. 758–763.